Journal of Power Sources 195 (2010) 6964–6969

Contents lists available at ScienceDirect

Journal of Power Sources

journal homepage: www.elsevier.com/locate/jpowsour

Polypyrrole/carbon aerogel composite materials for supercapacitor

Hongfang An[a], Ying Wang[b], Xianyou Wang[a,*], Liping Zheng[a], Xingyan Wang[a], Lanhua Yi[a], Li Bai[a], Xiaoyan Zhang[a]

[a] School of Chemistry, Key Laboratory of Environmentally Friendly Chemistry and Applications of Minister of Education, Xiangtan University, Hunan 411105, China
[b] School of Chemical Engineering and Pharmacy, Wuhan Institute of Technology, Hubei 430073, China

ARTICLE INFO

Article history:
Received 10 February 2010
Received in revised form 15 April 2010
Accepted 22 April 2010
Available online 29 April 2010

Keywords:
Carbon aerogel
Polypyrrole
Composite
Supercapacitor

ABSTRACT

Polypyrrole (PPy)/carbon aerogel (CA) composite materials with different PPy contents are prepared by chemical oxidation polymerization through ultrasound irradiation and are used as active electrode material for supercapacitor. The morphology of PPy/CA composite is examined by scanning electron microscopy (SEM) and transmission electron microscopy (TEM). The results show that PPy is deposited onto the surface of CA. As evidenced by cyclic voltammetry, galvanostatic charge/discharge test and EIS measurements, PPy/CA composites show superior capacitive performances to CA, moreover, the results based on cyclic voltammograms show that the composite material has a high specific capacitance of 433 F g^{-1}, while the capacitance of CA electrode is only 174 F g^{-1}. Although the supercapacitor used PPy/CA as active electrode material has an initial capacitance loss due to the instability of PPy, the specific capacitance after 500 cycles stabilizes nearly at a fixed value.

1. Introduction

Comparing with activated carbons (AC) and metal (hydro-) oxides, conductive polymers (CPs) are less expensive to use as the electrode materials of supercapacitor. The CPs have electrochemical characteristics of rapidly reversible doping and dedoping ability so that they can store the charge throughout the entire volume. Among several kinds of candidate CPs for the supercapacitor, such as polypyrrole (PPy), polyaniline (PANI), poly(3-methylthiopin) (PMET), poly(1,5-diaminoanthraquinon) (PDAAQ), poly(3,4-ethylenedioxythiopene) (PEDOT), PPy is an intrinsically CPs because of its high conductivity, high storage ability, good thermal and environmental stability, high redox and capacitive current and biocompatibility [1–5]. However, like most CPs, the PPy has a disadvantage of long-term cycle life instabilities than carbon-based electrodes because the redox sites in the polymer backbone are not sufficiently stable and the backbone of polymer can be destroyed within a limited number of charge/discharge cycles. Recently, in order to enhance the capacitance of carbon-based supercapacitor and improve the cycle life of PPy, some researchers used carbons as substrate materials to prepare composites, and there are a number of literature on PPy/carbon composite electrodes such as PPy with activated carbon [6], multi-wall carbon nano-tube [7–9], single wall carbon nano-tube [10], carbon foam [1], glassy carbon [11], carbon fiber [12] and graphite fiber matrix [13].

Carbon aerogel is a kind of novel mesoporous carbon materials with an electrically conductive carbon network, a low density, and other interesting properties [14–16]. It is reported that the PPy/carbon aerogel composite was used as photovoltaic materials [17], but there are few reports about the PPy/carbon aerogel composite as electrode material for supercapactor. In previous works, we studied preparation technology and electrochemical properties of carbon aerogel (CA) [18] and the composites of CA with RuO_2 [19], MnO_2 [20] and polyanline [21]. In this paper, we synthesized the PPy/CA composite using as active electrode materials of supercapacitor, the electrochemical performances of PPy/CA were evaluated by means of cyclic voltammetry (CV), the galvanostatic charge/discharge, electrochemical impedance spectroscopy (EIS).

2. Experimental

2.1. Synthesis of PPy/CA composite

CA was derived from pyrolysis of a resorcinol–formaldehyde gel. The procedure was reported in our previous study [18]. The molar ratio of formaldehyde (F) to resorcinol (R) was held at a constant value of 2:1. Na_2CO_3 (C) was added as the catalyst. During the preparation process, the R/C ratio was controlled to 1500.

The PPy/CA composites were prepared using sodium dodecyl sulfate (SDS) as the surfactant through chemical oxidation polymerization [12,22]. Fig. 1 shows a possible mechanism of PPy/CA composite formation in the presence of SDS. To prepare the PPy/CA composites, the procedure is followed as two steps. Firstly, 0.1 g

* Corresponding author. Tel.: +86 731 58292060; fax: +86 731 58292061.
E-mail address: wxianyou@yahoo.com (X. Wang).

0378-7753/$ – see front matter © 2010 Elsevier B.V. All rights reserved.
doi:10.1016/j.jpowsour.2010.04.074

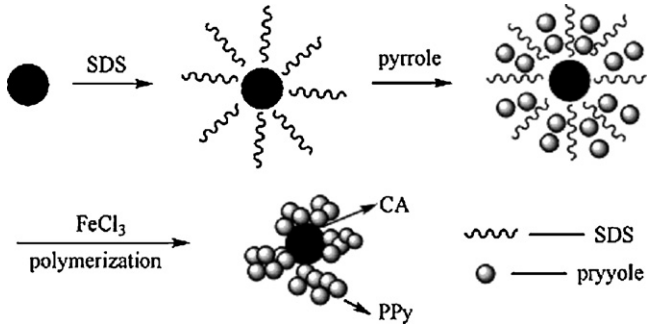

Fig. 1. A possible mechanism of PPy/CA composite formation.

CA was dispersed in 200 mL of distilled water solution containing 0.02 g SDS, and kept for ultrasound for about 10 min, and then stirred vigorously for about 2 h below 20 °C; subsequently, the solution was kept in refrigerator for about 5 min. Secondly, pyrrole monomer was added into the above solution according to 4 kinds of ratio (CA:pyrrole = 1:0.5, 1:1, 1:2, 1:4, and the weight of pyrrole monomer were 0.05 g, 0.1 g, 0.2 g, 0.4 g, respectively). Then $FeCl_3$, which was dissolved in 20 mL of distilled water as oxidant (the ratio of $FeCl_3$:pyrrole = 1:1), was added into the above solution to begin the polymerization reaction. The reaction was irradiated by ultrasonic wave for about 10 min and then stirred for about 2 h under 20 °C. The resulting PPy/CA composite precipitate was filtered and washed with water and ethanol several times until the filtrate was pellucid. Finally, the product was dried in vacuum at 50 °C for 12 h. In the PPy/CA composite, the content of PPy is 10%, 21%, 35%, and 63%, respectively, when the ratios of CA:pyrrole were 1:0.5, 1:1, 1:2, 1:4. Hereinafter, the name of PPy/CA composite was shortening as *x*-PPy/CA, where *x* delegates the content of PPy in the composite. For example, the content of PPy was 10%, we called it 10%-PPy/CA. The pure PPy was prepared by the same method without adding any CA.

2.2. Preparation of electrodes

The mixture containing 80 wt.% active material, 10 wt.% graphite, and 10 wt.% polytetrafluoroethylene (60%) was well mixed in N-methyl-2-pyrrolidone (NMP) until to form the slurry with proper viscosity, and then the slurry was uniformly laid on a Ni foam that used as a current collector (area was about 1.5 cm^2) and then dried at 50 °C for 24 h. The Ni foam coating PPy/CA composite was pressed for 1 min under 1.6×10^6 Pa. So, the PPy/CA composite electrode was well prepared.

2.3. Measurement

The FT-IR (Perkin Elicer Spectrum One) was used to confirm the polymerization of the PPy deposited on CA. To examine the surface morphology of the PPy/CA composite, the scanning electron microscopy (SEM, Hitachi S-3500N) and transmission electron microscopy (TEM, Tecnai G2) were used.

The electrochemical performances of the prepared electrodes were characterized by cyclic voltammogram (CV), charge/discharge tests and AC impedance using electrochemical analyzer systems (CHI 660A). The used electrolyte was 6 mol L^{-1} KOH solution. The experiments were carried out using a three-electrode cell, in which the Ni form and the Hg/HgO electrode were used as counter and reference electrodes, respectively. The symmetrical button supercapacitor was assembled according to the order of electrode–separator–electrode, and the cycle life was carried out by potentiostat/galvanostat (BTS 6.0, Neware, Guangdong, China) on button supercapacitor.

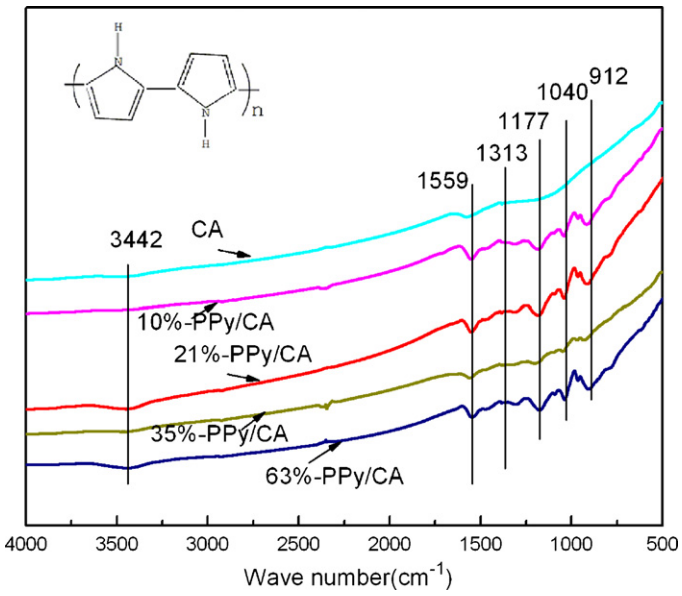

Fig. 2. FT-IR spectra of CA and PPy/CA composites.

3. Results and discussion

3.1. Structural characterization

Usually, PPy is made of alternate pyrrole ring as shown in Eq. (1).

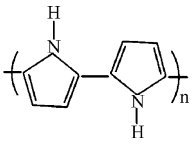

(1)

Fig. 2 is the FT-IR spectra of CA and PPy/CA. As shown in Fig. 2, 3442 cm^{-1} and 1559 cm^{-1} are attributed to the N–H and C=C stretching vibration of the PPy; 1177 cm^{-1} and 912 cm^{-1} indicate the doping state of PPy [23] and the peaks at 1040 cm^{-1} and 1313 cm^{-1} are attributed to C–H deformation and C–N stretching vibrations of the PPy, respectively. These peaks are all observed on the curves of PPy/CA composite, these data are similar to pure PPy. Whatever, on the curve of CA, these peaks are not observed, only the 1559 cm^{-1} which owes to the C=C can be found. It indicates that the Ppy/CA composites are successfully prepared. Meanwhile, the SEM and TEM images of the CA and 35%-PPy/CA composite are showed in Fig. 3. From Fig. 3a and c, it can be seen that the CA has the pearly network structure, and the sphere is smooth-faced. Compared with the 35%-PPy/CA composite (Fig. 3b), a great morphology change on the external surface of CA (in Fig. 3a) takes place, and the surface morphology becomes rough, indicating that the CA sphere has been coated with PPy. Besides, it can be seen from TEM images in Fig. 3c and d that the light morphologies come from the PPy and the dark core is CA.

3.2. Electrochemical characterization of PPy/CA composite

Cyclic voltammerty was used in the determination of the electrochemical proprieties of the PPy/CA composite. The CVs of PPy/CA composite electrodes are showed in Fig. 4. It can clearly be found that the CV of the CA electrode is mirror image symmetry, indicating the excellent electrochemical behavior, while the CV curve of PPy electrode is distorted from mirror image symmetry and a couple of peaks of oxidation and reduction are observed, suggesting that the reversibility of the PPy electrode is not good in the

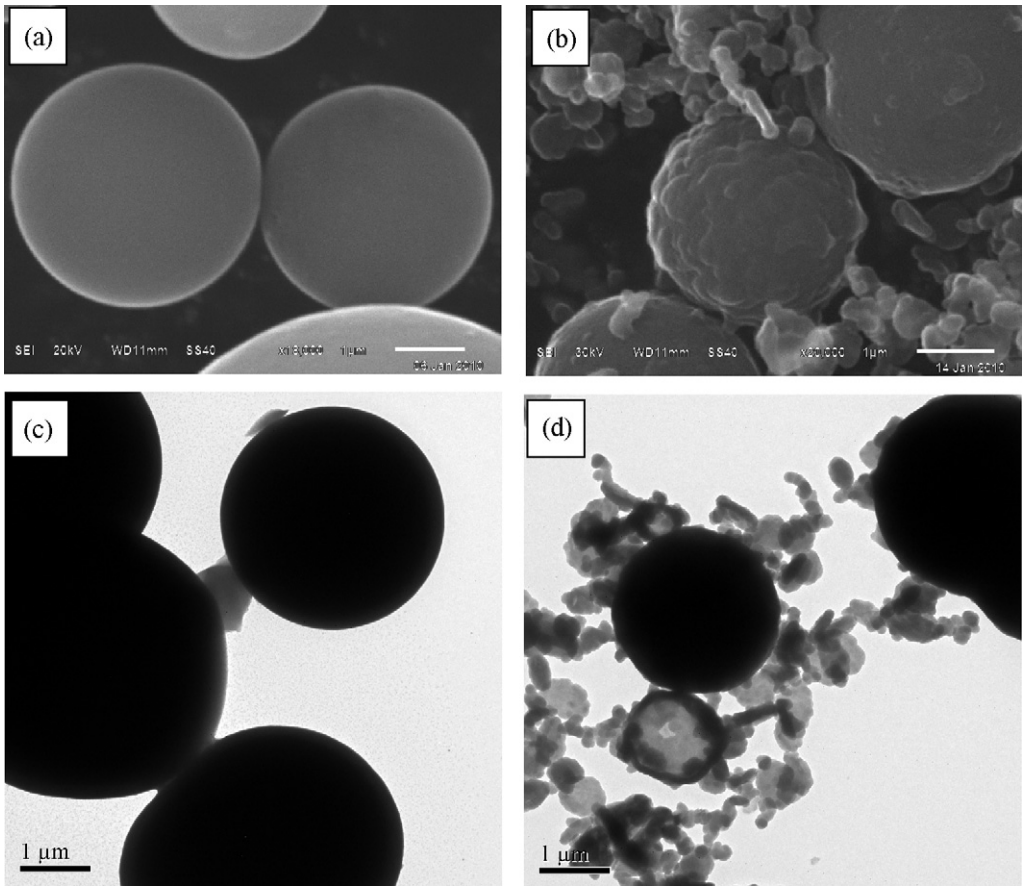

Fig. 3. SEM images of CA (a), 35%-PPy/CA composite (b) and TEM images of CA (c), 35%-PPy/CA composite (d).

scanning potential range. Meanwhile, Fig. 4 reveals that the capacitive characteristics of the PPy/CA composite electrode are distinct from CA electrode and close to the PPy electrode. Compared the CVs of PPy/CA, the oxidation and reduction peaks are observed on all of the PPy/CA composites. Therefore, it can be known that not only double-layer capacitances but also Faradic capacitances exist in the PPy/CA composite. Among all CV profiles, the oxidation and reduction peaks can be obviously seen, and the deviation of peak potential is least for the 35%-PPy/CA composite electrode.

To analyze the variation of capacitance with the scan rate, the CV measurement was carried out, and the specific capacitance of the electrode can be calculated by Eq. (2) [12] based on CV test.

$$C \equiv \frac{Q}{V} = \int \frac{idt}{\Delta V} \tag{2}$$

where i is a sampled current, dt is a sampling time span, and ΔV is the total potential deviation of the voltage window. Fig. 5 shows the

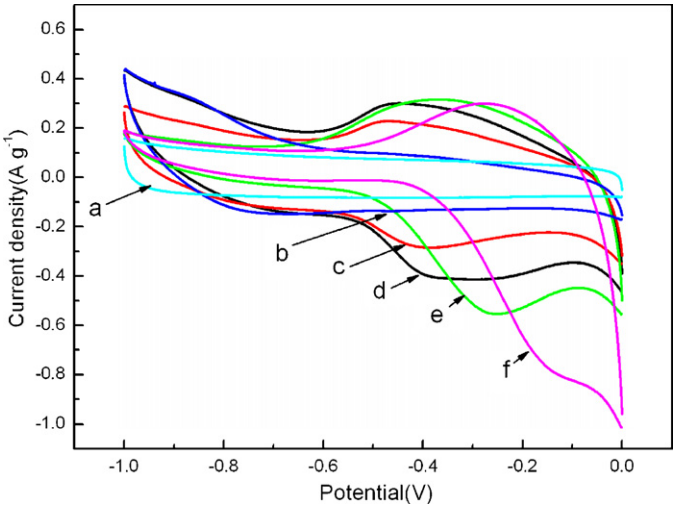

Fig. 4. Cyclic voltammograms at 2 mV s^{-1} of scan rate for the PPy/CA composite electrode with different contents of Ppy (a: CA, b: 10%-PPy/CA, c: 21%-PPy/CA, d: 35%-PPy/CA, e: 63%-PPy/CA, f: PPy).

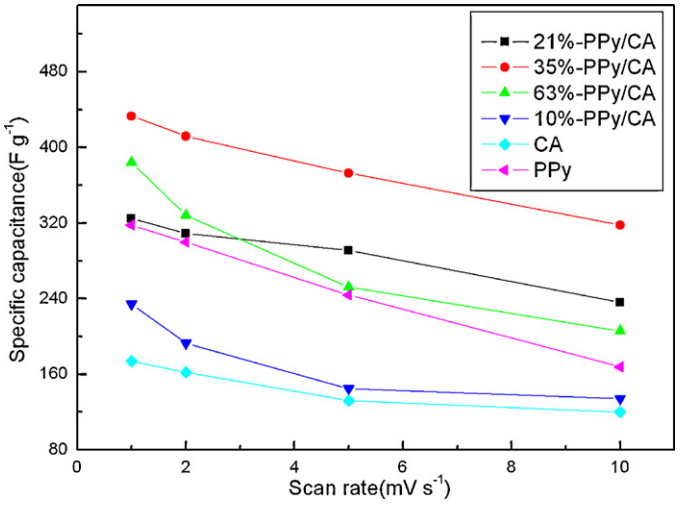

Fig. 5. The specific capacitances of CA, the PPy/CA composite and PPy electrodes.

specific capacitance variations of different PPy contents in PPy/CA composites with scan rate from 1 mV s^{-1} to 10 mV s^{-1}. There is an initial increase in the values of the specific capacitance with an increase in content of PPy. When the loading mass of PPy was 35%, the PPy/CA electrode (35%-PPy/CA) represents the highest specific capacitance with a slight decent even at higher scan rates. The specific capacitance of 35%-PPy/CA composite reaches to 433 F g^{-1}, 412 F g^{-1}, 373 F g^{-1} and 318 F g^{-1} at 1 mV s^{-1}, 2 mV s^{-1}, 5 mV s^{-1} and 10 mV s^{-1}, respectively, which is attributed to the combined effect of double-layer and redox capacitive behavior. Furthermore, the results in Fig. 5 indicate that all PPy/CA electrodes exhibit higher capacitance than the pure CA.

For more detail understanding pseudo-capacitive behavior of the PPy/CA composite, 35%-PPy/CA, 10%-PPy/CA and 63%-PPy/CA electrodes were examined by the CV at various scan rates of 1 mV s^{-1}, 2 mV s^{-1}, 5 mV s^{-1} and 10 mV s^{-1} as shown in Fig. 6. In Fig. 6a, the anodic and cathodic current peaks of the 35%-PPy/CA electrode are consistently increased as increasing scan rate up to 10 mV s^{-1} without significant increment of the peak current potential deviations. However, as shown in Fig. 6b, the anodic current peak and cathodic current peak of the 10%-PPy/CA electrode obviously weaken because the content of PPy in composite was low. In Fig. 6c, the obvious anodic and cathodic current peaks can be observed at low scan rates, with the increasing of scan rate, the peak potential difference is increased and the CVs become asymmetry. So, the reversibility of 63%-PPy/CA electrode becomes worse.

From above results, it is found that the 35%-PPy/CA has a good pseudo-capacitive behavior except double-layer capacitance, and its capacitance is apparently higher than 10%-PPy/CA and 63%-PPy/CA. And, it is notable that the 35%-PPy/CA has a better reversibility than 63%-PPy/CA. Hence, it is able to understand that the PPy content in the PPy/CA composites will play an important role for obtaining fully reversible and very fast redox behavior because PPy can contribute to the pseudo-capacitance of charge storage.

In order to examine the performance of the PPy/CA composite electrodes, the galvanostatic charge/discharge was carried out. As shown in Fig. 7, the galvanostatic charge/discharge curve of CA is almost linear and presents typical symmetrical triangle shape, indicating that CA has good double-layer capacitive behavior, and the curves of PPy was not ideal triangle shape due to existence of the Faradaic reactions. In comparison, the charge/discharge curves of PPy/CA composite electrode are similar to the PPy electrode, thus PPy/CA composite electrode will have much longer charge/discharge duration and an enhanced charge storage capacity than CA electrode. These phenomena are briefly attributed to pseudo-capacitance in the PPy oxidation–reduction process. In addition, it can be seen from Fig. 7 that the discharge time and the specific capacitance of 35%-PPy/CA are maximum. For further understanding electrochemical behavior of the PPy/CA composite, Fig. 8 gives the galvanostatic charge/discharge curves of 35%-PPy/CA composite electrode at various current densities.

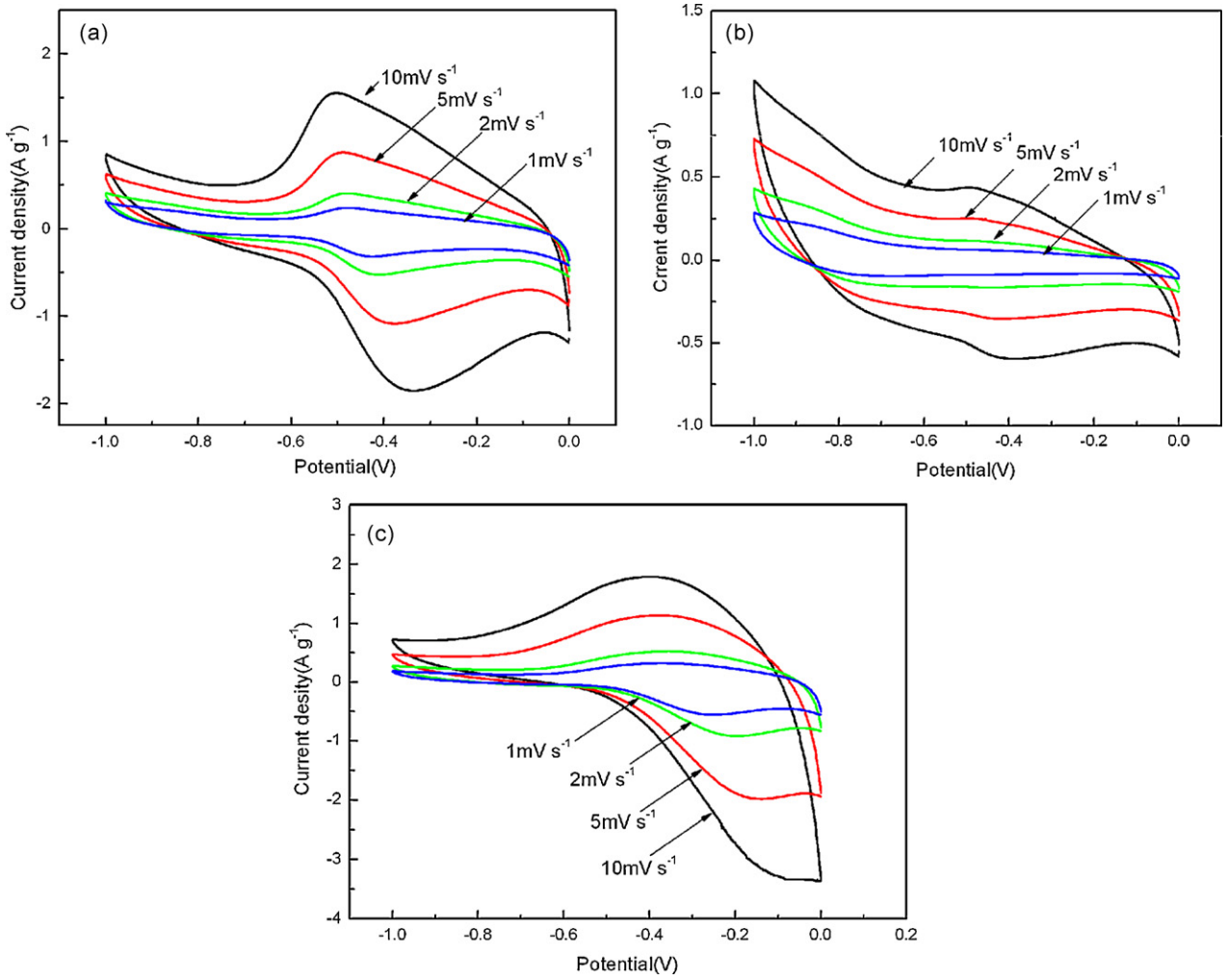

Fig. 6. Cyclic voltammograms of the 35%-PPy/CA (a), 10%-PPy/CA (b) composite electrode and 63%-PPy/CA (c) at different scan rates.

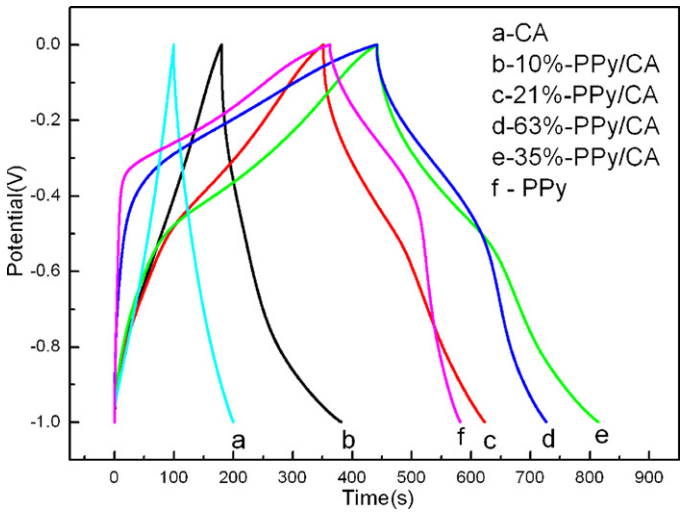

Fig. 7. The charge/discharge curves of CA, PPy/CA composite and PPy electrodes at 0.5 A g^{-1}.

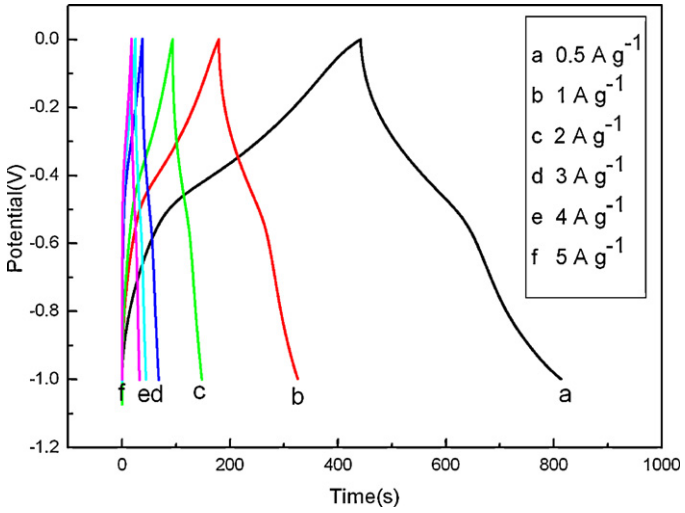

Fig. 8. The charge/discharge curves of 35%-PPy/CA composite electrode at different current densities.

In general, the specific capacitance of 35%-PPy/CA composite electrode decreases with the increasing of discharge current density, the reason is that the electrolyte ion cannot penetrate well into the inner of active materials due to slow diffusion at large current density.

Electrochemical impedance spectroscopy is a helpful experimental tool to characterize frequency response of supercapacitor. Experimental data extracted from this measurement are usually plotted in a Nyquist diagram which represents the imaginary part of the impedance vs. the real part. Fig. 9a represents the Nyquist plots obtained at open circuit potentials for AC, PPy/CA composite and PPy electrode. As being seen, the electrochemical resistance of the CA and all PPy/CA electrodes was small, whereas the electrochemical resistance of the pure PPy electrode was more, which indicates that the capacitive behaviors of CA and PPy/CA are much better than PPy. From the insert in Fig. 9a, a small depressed semicircle was observed in the high frequency region, which represents a parallel combination of resistive and capacitive components. In all electrodes, the charge-transfer resistance of 35%-PPy/CA was least, which is an important factor in the fast redox systems, especially for supercapacitors. A straight line can be seen in the low frequency, the straight line of 35%-PPy/CA composite electrode leans more towards imaginary axis, indicating that it has better capacitive behavior.

For supercapacitors, the majority of their capacitance is only available at low frequency, so attention should be paid that the impedance data are in this range [24]. Fig. 9b presents the conversion capacitance obtained from electrode impedance of CA and PPy/CA composite electrodes. The capacitance values were obtained from the following Eq. (3) [25]:

$$C = -\frac{1}{2\pi f Z''} \tag{3}$$

Here, C is the capacitance, f is the frequency, Z'' is the imaginary part of impedance. When the frequency increases, the capacitance of all samples decreases, and at high frequency region the supercapacitors behave like a pure resistance, which indicates that the electrolyte ions cannot penetrate into micropores under high frequencies. It is found that all PPy/CA composites have higher capacitance than CA electrode, and 35%-PPy/CA gives the highest capacitance at low frequency range; it is in consistent with CV and galvanostatic charge/discharge data. It should be noted that the specific capacitances value of all samples at 0.01 Hz are different from those derived form CV test and constant-current discharges, which is mainly due to the different testing systems applied.

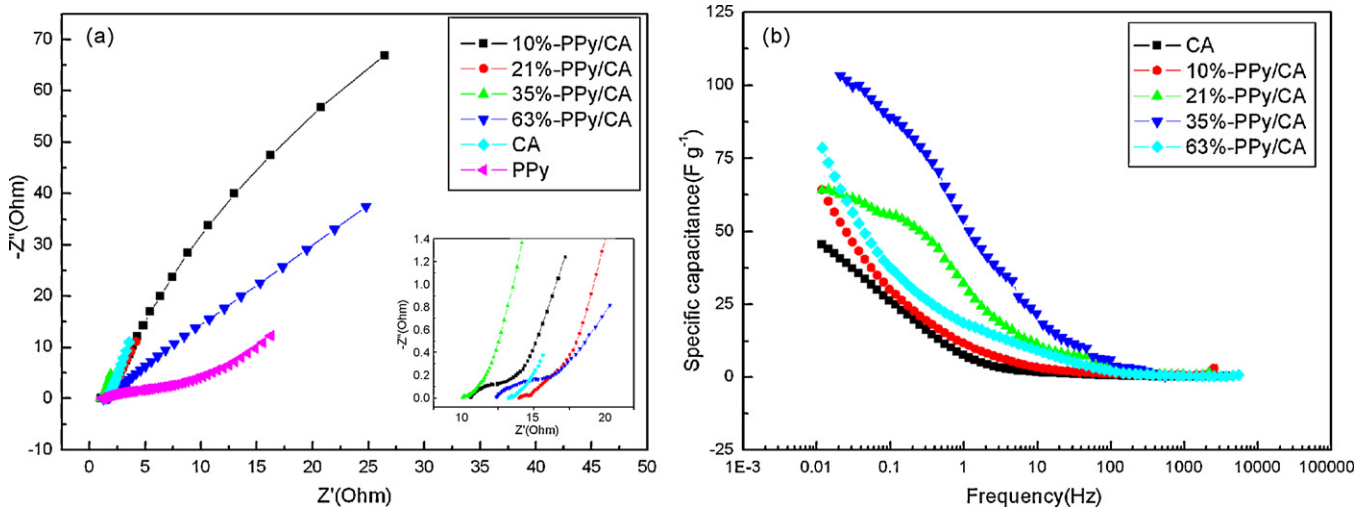

Fig. 9. (a) Nyquist plot of CA, PPy/CA composite and PPy electrodes. (b) Capacitance vs. frequency plots of the CA and PPy/CA composite electrodes.

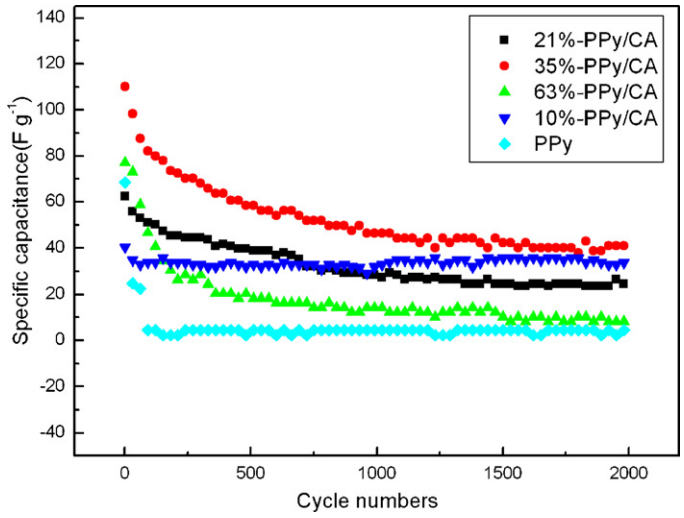

Fig. 10. Cycle life of PPy/CA composite and PPy supercapacitors under current density of 1 A g^{-1}.

The cycle life is another important factor for the supercapacitor, so the cycle life of the PPy/CA composite supercapacitor was measured using Neware test system. The cycle life curves of the supercapacitors at the current density of 1 A g^{-1} are illustrated in Fig. 10. From Fig. 10, the specific capacitance of PPy supercapacitor reaches 70 F g^{-1}, but the loss of capacitance is apparently high. Although the loss of PPy/CA composite supercapacitor is large at initial cycles due to the instability of PPy, but after 500 cycles the specific capacitance stabilized at a fixed value. Hence, the composites have better long-term cycle life than the PPy. Especially, the 35%-PPy/CA supercapacitor exhibits the highest specific capacitance and the 10%-PPy/CA shows the best stability among all PPy/CA supercapacitor. But the specific capacitance of 10%-PPy/CA is clearly low. So it is believed that the 35%-PPy/CA has much better electrochemical performance.

4. Conclusions

(1) Various contents of PPy/CA composite materials were synthesized successfully by chemical oxidation polymerization through ultrasound irradiation. The as-prepared PPy/CA composite materials have a pearly network structure like CA and its surface was apparently rough.

(2) The PPy/CA composites do not only process double-layer capacitance but also have pseudo-capacitance and the specific capacitances of all the PPy/CA composites are higher than CA.

(3) It has been found that the optimum amount PPy in PPy/CA composite is 35 wt.%. The specific capacitance of the 35%-PPy/CA composite electrode in 6 mol L^{-1} KOH electrolyte is approximately 433 F g^{-1}. Besides, the 35%-PPy/CA composite has a small electrochemical resistance and good cyclic performance. Although capacitance of PPy/CA composite button supercapacitor has decay at initial cycles due to the instability of PPy, but after 500 cycles the specific capacitance stabilized at a fixed value, indicating that the cycle stability is better than PPy. Hence, it is notable that preparing composite was an effective way to enhance the capacitance of carbon materials and improve the cycle life of conductive polymer.

Acknowledgements

This work was financially supported by the Natural Science Foundation of China (Grant No. 20871101), Key Project of Science and Technology of Hunan Province Government (Grant No. 2009WK2007) and Research Fund for the Doctoral Program of Higher Education of China (Grant No. 2094301110005).

References

[1] Q. Wu Zhang, X. Zhou, H.-S. Yang, J. Power Sources 125 (2004) 141.
[2] H.C. Kang, K.E. Geckeler, Polymer 41 (2000) 6931.
[3] A. Laforgue, P. Simon, C. Sarrazin, et al., J. Power Sources 80 (1999) 142.
[4] J.Y. Lee, D.Y. Kim, C.V. Kim, Synth. Met. 74 (1995) 103.
[5] K. Hycok, A.K. Ku, J. Jeong, et al., J. Electrochem. Soc. 149 (2002) A1058.
[6] B. Muthulakshmi, D. Kalpana, S. Pitchumani, et al., J. Power Sources 158 (2006) 1533.
[7] K. Jurewicz, S. Delpeux, V. Bertagna, et al., Chem. Phys. Lett. 347 (2001) 36.
[8] Q. Xiao, X. Zhou, Electrochim. Acta 48 (2003) 575.
[9] V. Khomenko, E. Frackowiak, F. Beguin, Electrochem. Acta 50 (2005) 2499.
[10] K.H. An, K.K. Jeon, J.K. Heo, et al., J. Electrochem. Soc. 149 (2002) 1058.
[11] C.M. Li, C.Q. Sun, W. Chen, et al., Surf. Coat. Technol. 198 (2005) 474.
[12] J.H. Kim, Y.S. Lee, A.K. Sharma, Electrochim. Acta 52 (2006) 1727.
[13] J.H. Park, J.M. Ko, O.O. Park, et al., J. Power Sources 105 (2002) 20.
[14] N. Liu, S.T. Zhang, R. Fu, et al., Carbon 44 (2006) 2430.
[15] S.J. Kim, S.W. Hwang, S.H. Hyun, J. Mater. Sci. 40 (2005) 725.
[16] T.F. Baumann, M.A. Worsley, T.Y.J. Han, et al., J. Non-Cryst. Solids 354 (2008) 3513.
[17] P.H. Kim, J.D. Kwon, J.S. Kim, Synth. Met. 142 (2004) 153.
[18] J. Li, X.Y. Wang, Q.H. Huang, J. Power Sources 158 (2006) 784.
[19] J. Li, X.Y. Wang, Q.H. Huang, J. Appl. Electrochem. 37 (2007) 1129.
[20] J. Li, X.Y. Wang, Q.H. Huang, et al., J. Power Sources 160 (2006) 1501.
[21] H.F. An, X.Y. Wang, Y. Wang, J. Solid State Electrochem. 14 (2010) 651.
[22] X.F. Lu, H. Mao, W.J. Zhang, Polym. Compos. 30 (2009) 847.
[23] S.T. Selvan, Chem. Commun. 3 (1998) 351.
[24] B.P. Bakhmatyuk, B.Y. Venhryna, I.I. Grygorchaka, et al., J. Power Sources 180 (2008) 890.
[25] K.S. Ryu, Y.G. Kee, K.M. Kim, et al., Synth. Met. 153 (2005) 89.